Asian Journal of Scientific Research, 2013
ISSN 1992-1454 / DOI: 10.3923/ajsr.2013.

Preliminary Study of Thermoelectric System for Simultaneous Heating and Cooling

[1]How Meng Git, [2]Ong Kok Seng, [1]Syed Ihtsham-ul-Haq Gilani and [1]M. Shiraz B. Aris
[1]Department of Mechanical Engineering, Universiti Teknologi PETRONAS, Bandar Seri Iskandar, 31750 Tronoh, Malaysia
[2]School of Engineering, Monash University Sunway Campus, Jalan Lagoon Selatan, Selangor, Malaysia

Corresponding Author: How Meng Git, Department of Mechanical Engineering, Universiti Teknologi PETRONAS, Bandar Seri Iskandar, 31750 Tronoh, Malaysia

ABSTRACT

The simultaneous heating and cooling ability of thermoelectric modules has neither been researched widely nor commonly exploited either in an industrial or domestic level. This paper presents the preliminary experiments of a thermoelectric system for simultaneous heating and cooling. The objective of the study is to determine the performance of the system that can potentially be used to produce hot and cold water simultaneously. The system's main test section comprises of an array of ten thermoelectric modules arranged electrically in parallel and sandwiched between two rectangular aluminum water channels as heat exchangers. The variables are input power to the thermoelectric modules and flow rates in the water channels. Temperature measurements were recorded for both hot and cold surfaces of the thermoelectric modules and the water in the channels. Results obtained indicated significant influence of input current on the performance of the system. However, the high water flow rates employed in the study had minimal effect. Discussions are presented on possible approaches to improve the system performance to achieve an acceptable level for practical usage.

Key words: Thermoelectric heating, thermoelectric cooling, simultaneous heating and cooling

INTRODUCTION

Applications of thermoelectric (TE) devices cover an extensive area, ranging from military, aerospace, automobile, telecommunications, scientific and laboratory instruments and consumer products (Goldsmid, 1995; Redstal and Studd, 1995; Davis *et al*., 2006). Commercial single-stage TE modules cover a wide range of face sizes from 1.8×3.4 to 62×62 mm^2 and heights from 2.45 to 5.8 mm, with maximum cooling power from 0.2 to 125 W (Uemura, 1995). Multi-stage modules may be used to increase total heat pump performance. Large-scale applications involving cooling powers greater than several kilowatts have been built for specialized applications such as air conditioning of parked aircraft, trains, automobiles, submarines and large containers (Stockholm, 1995).

A few recent studies showcase some interesting works related to TE system. Khire *et al*. (2005) and Xu *et al*. (2007) introduced a new enclosure technology that integrates photovoltaic and TE technologies. The technology is called the active building envelope system. Solar radiation is converted into electrical energy by a PV system and subsequently used to power a TE system for cooling in summer and heating in winter. When operating in heating mode, the hot side

temperature could reach up to 60°C with an ambient temperature of about 20°C. In cooling mode, the cold side temperature dropped close to 15°C with the ambient temperature of about 20°C. This might not be sufficient to satisfy cooling requirements during summer months. The performance of the TE system can be improved by improving the heat dissipation ability of the heat sink. Lertsatitthanakorn *et al.* (2008) investigated the cooling performance and thermal comfort of a TE ceiling cooling panel system. A suitable condition occurred at 1.5 A of input current with a corresponding cooling capacity of about 289.4 W, giving a COP of 0.75 with average indoor temperature of 27°C.

The performance of thermoelectric device is governed by the figure of merit of the thermoelectric material, Z, defined by:

$$Z=\frac{\alpha}{\rho k} \quad (1)$$

where, α is the Seebeck coefficient, r is the electrical resistivity and k is the thermal conductivity of the thermoelectric material.

According to Lewis *et al.* (2007), current research on thermoelectric materials is aimed at improving the figure of merit by reducing the lattice thermal conductivity and is concentrated in two areas: (1) finding new compounds exhibiting phonon glass-electronic crystal characteristics with favourable properties and (2) producing thermoelectric materials using low dimensional structure (quantum wells, quantum wires, quantum dot and superlattices). Useful information and discussions on research of thermoelectric materials can be referred to Goldsmid and Nolas (2001) and Slack (1995). A recent article by Bigdilu and Zadeh (2012) provided the theory of size and temperature dependence of thermoelectric figure of merit in low-dimensional bismuth telluride semiconductor crystals.

The simultaneous heating and cooling ability of TE modules can be utilized to produce hot and cold water at the same time. A potential application may be producing domestic hot water for bath while delivering cold water for air cooling. This paper reports a preliminary investigation of a basic TE system to produce hot and cold water simultaneously. The objective of the present investigation is to determine the performance of a TE system for simultaneous heating and cooling in terms of Coefficient of Performance (COP) and water temperature difference.

THEORETICAL MODEL

Figure 1 shows the heat transfer components at the hot and cold junctions of a TE module. Heat transfer due to Peltier effect at the cold side is given by Eq. 2.

$$q_{pelt} = 2\,\alpha\,N_{TE}\,I\,T_c \quad (2)$$

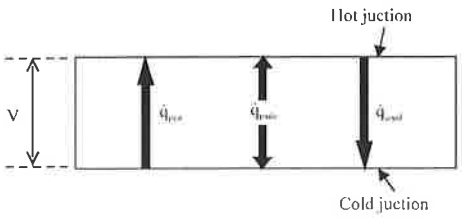

Fig. 1: Heat transfer components at the hot and cold junctions of a TE module

Heat transfer due to Joule effect is given by Eq. 3:

$$\dot{q}_{joule} = \frac{2\rho_{TE} N_{TE} I^2}{G} \tag{3}$$

Heat transfer due to temperature difference between hot and cold junctions is given by Eq. 4:

$$\dot{q}_{cond} = k_{TE} N_{TE} G \Delta T \tag{4}$$

Using the energy balance approach, the net heat transfer rate at the cold and hot junctions are expressed, respectively, by Eq. 5 and 6:

$$q_c = 2N_{TE}\left[\underbrace{\alpha I T_c}_{\text{Peltier effect}} \underbrace{-\frac{\rho_{TE} I^2}{2G}}_{\text{Joule effect}} \underbrace{-k_{TE} G \Delta T}_{\text{Conduction}}\right] \tag{5}$$

$$q_h = 2N_{TE}\left[\alpha I T_h + \frac{\rho_{TE} I^2}{2G} - k_{TE} G \Delta T\right] \tag{6}$$

The electrical power input is obtained using Eq. 6:

$$P = IV \tag{7}$$

The coefficient of performance for cooling and heating are calculated by Eq. 7 and 8, respectively:

$$COP_c = \frac{q_c}{P} \tag{8}$$

$$COP_h = \frac{q_h}{P} \tag{9}$$

MATERIALS AND METHODS

The schematic of the experimental setup of the TE system is shown in Fig. 2. The experimental setup comprises of two pumps, two ball valves, two flow meters and a test section. The test section consists of a single row of ten TE modules (CP1.4-127-10L by Laird), connected electrically in parallel, while being sandwiched by water channels on the top and bottom. Each TE module measures 40×40×4.7 mm. Manufacturer's data shows the maximum cooling capacity of 36.7 W at 3.9 A with hot side temperature 50°C. The water channels are made from aluminum with outer dimensions of W50 mm×H25.4 mm×L1070 mm and thickness of 3.18 mm. A DC power supply (GW GPR 1850HD) provides the power to the TE modules. Water is circulated in parallel direction through the channels via two pumps and their flow rates adjusted individually by ball valves. In the top channel, water heats up by absorbing heat from the hot junction of TE modules before exiting. In the bottom channel, the water gets chilled by the cold junction of TE modules before

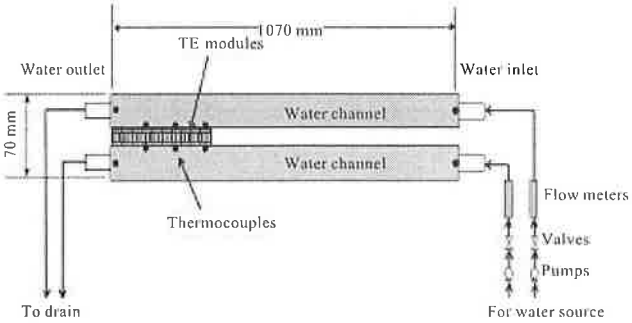

Fig. 2: Schematic of experimental setup

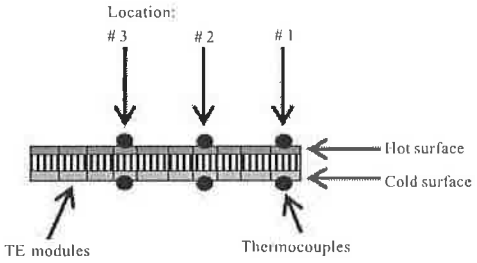

Fig. 3: Close-up view of TE modules and attached thermocouples

exiting. In essence, the test section functions as a water heater and cooler at the same time. Temperature measurements are made using T-type thermocouples (±0.5°C) and data is recorded with a data logger (Graphtec GL800-AS) set to record data every second. To measure the TE surface temperatures, two thermocouples are placed in contact with the surface of the hot and cold surfaces of individual module at the locations indicated in Fig. 2. A close-up view of the array of TE modules and the attached thermocouples is shown in Fig. 3. Additionally, two thermocouples are inserted at both ends of the water channels to record the inlet and outlet water temperatures of each channel.

The water flow rates are fixed at 1.0, 1.5 and 2.0 lpm for each of the four power settings. The input power is calculated using Eq. 7. Temperature responses of the TE module surfaces and the water are recorded upon reaching steady state when the temperatures remain relatively constant over time. Each set of data contains one hundred continuous readings with one second interval. The final temperature is then calculated by averaging the set of one hundred readings.

RESULTS AND DISCUSSIONS

The summary of results is tabulated in Table 1. Each value of the water temperatures ($T_{wh,i}$, $T_{wh,o}$, $T_{wc,i}$ and $T_{wc,o}$) is averaged from one hundred readings after attaining steady state. The coefficient of performance (COP_h and COP_c) are determined using Eq. 8 and 9, respectively. Table 2 displays the TE surface temperatures for the three locations indicated in Fig. 3. The currents indicated are averaged from the ten TE modules.

The average input current for each TE module are set at 0.5 to 2.0 A, with 0.5 A intervals. For each current setting, the water flow rates are varied at 1.0, 1.5 and 2.0 lpm. The system is

Table 1: Summary of experimental results with calculated COP for heating and cooling

		Water temperature in hot channel (°C)			Water temperature in cold channel (°C)			COP_h	
Power (W)	Flow rate (lpm)	$T_{wh,i}$	$T_{wh,o}$	ΔT_{wh}	$T_{wc,i}$	$T_{wc,o}$	ΔT_{wc}	COP_h	COP_c
1.3	1.0	24.6	24.9	0.3	25.0	24.8	0.2	3.95	3.11
1.3	1.5	25.2	25.4	0.2	25.4	25.3	0.1	4.00	3.17
1.3	2.0	25.7	25.9	0.2	25.9	25.8	0.1	4.07	3.24
5.6	1.0	23.8	24.5	0.7	23.9	23.5	0.4	2.10	1.29
5.6	1.5	23.9	24.4	0.5	24.2	24.0	0.2	2.12	1.31
5.6	2.0	24.1	24.5	0.4	24.4	24.2	0.2	2.14	1.34
13.5	1.0	24.5	26.2	1.7	24.7	24.5	0.2	1.44	0.68
13.5	1.5	25.0	26.0	1.0	25.1	25.0	0.1	1.45	0.69
13.5	2.0	25.4	26.1	0.7	25.5	25.3	0.2	1.46	0.71
25.9	1.0	25.9	28.0	2.1	26.0	25.9	0.1	1.11	0.39
25.9	1.5	26.0	27.6	1.6	26.1	26.1	0.0	1.11	0.40
25.9	2.0	26.0	27.1	1.1	26.2	26.2	0.0	1.12	0.41

Table 2: TE surface temperatures at different locations along water channels (flow rate = 1.0 lpm)

	TE surface temperature (°C)							
	T_h				T_c			
Location	I = 0.5 A	I = 1.0 A	I = 1.5 A	I = 0.5 A	I = 0.5 A	I = 1.0 A	I = 1.5 A	I = 1.5 A
1	28.4	32.2	39.4	49.7	20.7	16.6	15.3	15.9
2	31.9	39.9	51.5	65.3	21.6	18.9	19.3	21.7
3	34.9	46.6	43.3	83.3	22.5	20.7	22.2	25.9

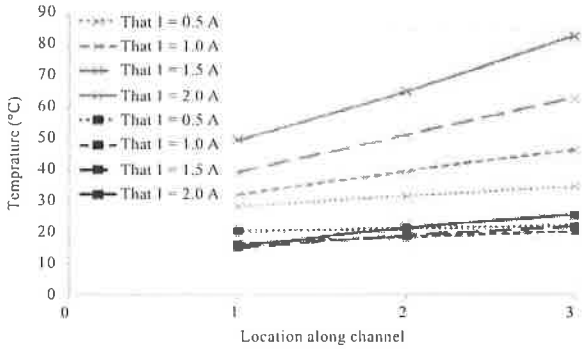

Fig. 4: TE surface temperatures at different locations along water channels (flow rate = 1 lpm)

allowed to reach steady state (approximately 5 min) before measurements are recorded at an interval of one second for a total of one hundred seconds.

Figure 4 shows the resultant TE surface temperatures at different locations along the water channel. The gradient of the slope of the line at the hot side is larger, subsequently, the surface temperature difference (ΔT) widens in the direction from water inlet to outlet. As the water temperature rises from location 1 to 3 in the hot channel, the TE module hot surface temperature rises in tandem as a result of reduced rate of heat transfer to the flowing water. On the cold side,

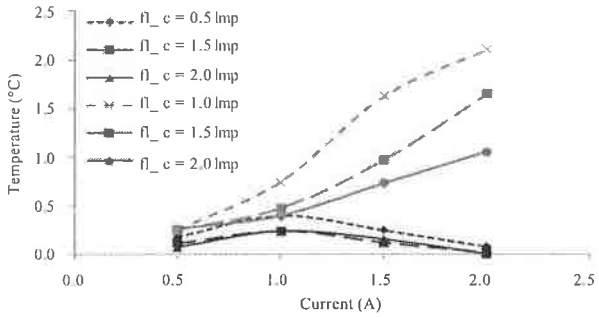

Fig. 5: Relationship between water temperature difference and input current for selected flow rates

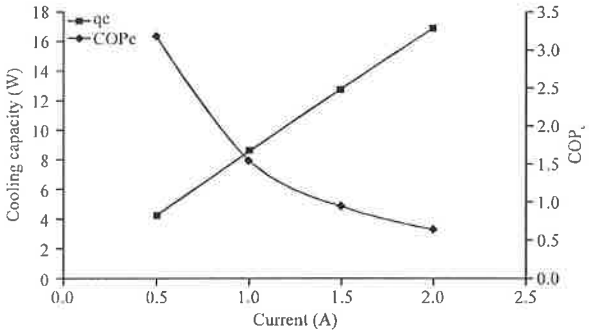

Fig. 6: Effect of input current on cooling capacity and COP for cooling

TE module surface temperature increases due to increased rate of conduction heat transfer from the hot surface. Consequently, the cooling performance drops as conduction heat becomes more prominent. With constant input voltage and different ΔT, current drawn by the array of TE modules is therefore non-uniform. This finding prompts further study on the characterization of individual TE modules used in the experiments. Temperature-dependent properties such as the Seebeck coefficient, electrical resistivity and thermal conductivity need to be determined in order to generate more accurate results using the theoretical model.

Figure 5 shows the effect of input current and water flow rate on the water temperature difference between the inlet and outlet of the hot and cold water channels. The top three lines represent the temperatures within the hot water channel, while the bottom three lines represent the temperatures within the cold water channel. The graph suggests that for the hot side, ΔT_{wh} increases with increasing current, while the opposite is true for cold side. There is an increase of water temperature difference between 0.5 and 1.0 A with T_{wc} peaks at 1.0 A for cold side. As input current is increased further, the cooling capacity drops due to the combination of greater Joule heating and conduction effect. Water temperature difference is largest at the lowest flow rate (1 lpm) for both hot and cold sides. Lower flow rates result in lower convective heat transfer along the channels, allowing for better local heat transfer to and from TE module cold and hot surfaces, respectively. The findings are in good agreement with a previous work by Kazmierczak *et al.* (2009).

Cooling capacity or cooling rate ($\dot{q}_c$) increases while COP_c decreases more significantly with current, as shown in Fig. 6. COP_c approaches a plateau as current is increased. Comparison with

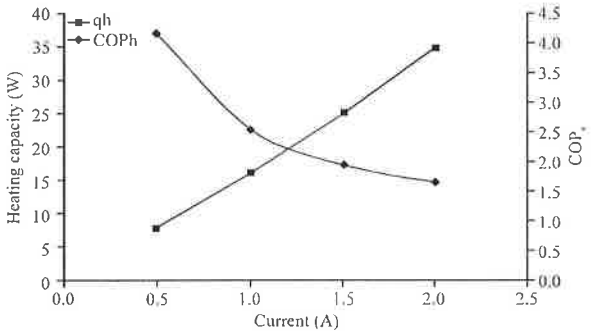

Fig. 7: Effect of input current on heating capacity and COP for heating

a previous research shows similar trends for both $\dot{q}_c$ and COP_c. Values differ due to different specification of TE modules used, experimental setting and heat sink designs. The graphs of $\dot{q}_h$ and COP_h (Fig. 7) display the same trends as the cold side with augmented values, indicating TE modules perform more effectively as a heater than as a cooler. As input current increases, the Joule heating becomes more prominent, therefore, augmenting the heating capacity. At the same time, the conduction effect is enhanced as the temperature difference between the hot and cold junctions increases.

CONCLUSION

This study presents the preliminary results of experiments conducted on a TE system for simultaneous cooling and heating. It was found that:

- Within the range of input current and flow rates under study, the TE system performs more efficiently as a heater than as a cooler. The maximum COP for heating was 4.07 while maximum COP for cooling was 3.24, both achieved at the input power of 1.3 W and flow rate of 2 lpm
- Temperature difference across the TE modules (ΔT) widens in the direction from water inlet to outlet, indicative of non-uniform current distribution to the TE modules. Characterization of the TE modules is important to determine the key properties to ensure more accurate results from the theoretical model
- At the hot side, maximum water temperature difference between inlet and outlet was 2.1°C. At the cold side, the water temperature differences were no more than 0.4°C between inlet and outlet. In order to produce an appreciable and useful temperature difference, future work needs to focus on improving heat transfer from TE module surfaces to the water
- While input power has a significant effect, the high water flow rates employed have minimal effect on the performance of the system. TE module surface temperatures are not significantly affected by the range of flow rates in the study. Further investigations are required by reducing the water flow rates and to vary the flow rates between the hot and cold channels in order to effectively reduce T_h and ΔT

ACKNOWLEDGMENT

The research is funded by Universiti Teknologi PETRONAS under STIRF CODE NO: 15/10.11.

NOMENCLATURE

COP	=	Coefficient of performance
G	=	Geometric property of TE module (m)
I	=	Current (A)
k	=	Thermal conductivity of TE material (W/m K)
k_{TE}	=	Thermal conductivity of TE module (W/m K)
P	=	Input power (W)
N_{TE}	=	Number of thermocouples in a TE module
$\dot{q}$	=	Heat transfer rate (W)
T	=	Temperature (°C or K)
TE	=	Thermoelectric
V	=	Voltage (V)
Z	=	Figure of merit (K^{-1})
α	=	Seebeck coefficient of TE material (V/K)
Δ	=	Difference in value
r	=	Electrical resistivity of TE material (Ω)
ρ_{TE}	=	Electrical resistivity of TE module (Ω m)
c	=	Cold side
h	=	Hot side
i	=	Inlet
joule	=	Joule
cond	=	Conduction
o	=	Outlet
pelt	=	Peltier
TE	=	Thermoelectric
w	=	Water

REFERENCES

Bigdilu, A.A.J. and H.H. Zadeh, 2012. Investigation of temperature dependence thermoelectric figure of merit (ZT) in Low-dimensional Bi_2Te_3. J. Applied Sci., 12: 863-869.

Davis, M.C., B.P. Banney, P.T. Clarke, B.R. Manners and R.M. Weymouth, 2006. Thermoelectric Refrigeration for Mass-Market Applications. In: Thermoelectrics Handbook: Macro to Nano, Rowe, D.M. (Ed.). CRC Press, UK.

Goldsmid, H.J. and G.S. Nolas, 2001. A review of the new thermoelectric materials. Proceedings of the 20th International Conference on Thermoelectrics, June 2001, Beijing, China, pp: 1-6.

Goldsmid, H.J., 1995. Applications of Thermoelectric Cooling. In: CRC Handbook of Thermoelectrics, Rowe, D.M. (Ed.). CRC Press, USA., pp: 617-620.

Kazmierczak, M.J., S. Krishnamoorthy and A. Gupta, 2009. Experimental testing of a thermoelectric-based hydronic cooling and heating device with transient charging of sensible thermal energy storage water tank. J. Thermal Sci. Eng. Appl., 1: 1-14.

Khire, R.A., A. Messac and S. van Dessel, 2005. Design of thermoelectric heat pump for active building envelope systems. Int. J. Heat Mass Transfer, 48: 4028-4040.

Lertsatitthanakorn, C., W. Srisuwan and S. Atthajariyakul, 2008. Experimental performance of a thermoelectric ceiling cooling panel. Int. J. Energy Res., 32: 950-957.

Lewis, J.S., I. Chaer and S.A. Tassou, 2007. Fostering the development of technologies and practices to reduce the energy inputs into the refrigeration of food-Reviews of alternative refrigeration technologies. Technical Report, Centre of Energy and Built Environment Research, School of Engineering and Design, Brunel Univeristy.

Redstal, R.M. and R. Studd, 1995. Reliability of Peltier Coolers in Fiber-Optic Laser Packages. In: CRC Handbook of Thermoelectrics, Rowe, D.M. (Ed.). CRC Press, USA., pp: 641-646.

Slack, G.A., 1995. New Materials and Performance Limits for Thermoelectric Cooling. In: CRC Handbook of Thermoelectrics, Rowe , D.M. (Ed.). CRC Press, USA., pp: 407-440.

Stockholm, J.G., 1995. Large-scale Cooling: Integrated Thermoelectric Element Technology. In: CRC Handbook of Thermoelectrics, Rowe, D.M. (Ed.). CRC Press, USA., pp: 657-666.

Uemura, K., 1995. Commercial Peltier Modules. In: CRC Handbook of Thermoelectrics, Rowe , D.M. (Ed.). CRC Press, USA., pp: 621-632.

Xu, X., S. van Dessel and A. Messac, 2007. Study of the performance of thermoelectric modules for use in active building envelopes. Build. Environ., 42: 1489-1502.